



Shahid Chamran
University of Ahvaz

Journal of Applied and Computational Mechanics



Research Paper

Lamb Wave Analysis in Anisotropic Multilayer Piezoelectric-piezomagnetic Material

Hamdi Ezzin¹, Mohamed Mkaoir², Zhenghua Qian³, Mohammad Arefi⁴, Raj Das⁵

¹ State Key Laboratory of Mechanics and Control of Mechanical Structures, Nanjing University of Aeronautics and Astronautics, 29 Yudao Jie, Nanjing, 210016, China, Email: ezzinhamdi@nuaa.edu.cn, ezzinhamdi@yahoo.fr

² Laboratory of Physics of Materials, Faculty of Sciences of Sfax, Route de la Soukra km 3.5, Sfax, 1171 3000, Tunisia, Email: mohamedmkaoir12@gmail.com

³ State Key Laboratory of Mechanics and Control of Mechanical Structures, Nanjing University of Aeronautics and Astronautics, 29 Yudao Jie, Nanjing, 210016, China, Email: qianzh@nuaa.edu.cn

⁴ Department of Solid Mechanics, Faculty of Mechanical Engineering, University of Kashan, Kashan, 87317-51167, Iran, Email: arefi63@gmail.com

⁵ Aerospace Engineering and Aviation, School of Engineering, RMIT University, Plenty Road, Victoria, 3082, Australia, Email: raj.das@rmit.edu.au

Received August 04 2021; Revised December 06 2021; Accepted for publication December 06 2021.

Corresponding authors: H. Ezzin (ezzinhmd@nuaa.edu.cn); Z. Qian (qianzh@nuaa.edu.cn)

© 2021 Published by Shahid Chamran University of Ahvaz

Abstract. The dynamic response of an anisotropic multilayer magneto-electro-elastic (MEE) plate due to an external excitation is investigated in this work, using the stiffness matrix approach. A parametric study is performed by varying the stacking sequence, polarization direction, boundary conditions, and interlayer thickness. The proposed method yields the numerical estimation of the dispersion curve and the free vibration of the Lamb waves for different crystallographic orientations and magneto-electric boundary conditions. It is demonstrated that the anisotropy highly affects the dispersion curve and the non-dimensional frequency, and also decreases the interlayer thickness of the magneto-electro-elastic multilayer and raises the phase velocity of the fundamental symmetric Lamb mode vibration. The key outcomes of this research can serve as a reference in the design and analysis of new smart magneto-electro-elastic structures.

Keywords: Lamb waves; Anisotropic materials; Multilayer piezoelectric/piezomagnetic material; Natural frequency; Dispersion curve.

1. Introduction

When using Lamb waves for inspecting materials, particularly multilayer piezoelectric-piezomagnetic materials in the present case, it is necessary to know the behavior of the material in question. The dispersion curves are thus essential since they enable us to know the phase and group velocities of the waves as a function of the frequency of the wave generated as well as the thickness of the plate under inspection. Smart materials respond to the externally applied field and are found to be very sensitive to multiple fields like electric, magnetic and elastic fields. Among them, magneto-electro-elastic (MEE) materials have captured the attention of the research community due to their high energy conversion capacity. Magneto-electro-elastic (MEE) materials are increasingly being researched because they provide an additional feature of electric/magnetic control of magnetization/polarization. MEE materials are a new category of materials possessing simultaneously ferroelectric and ferromagnetic properties exhibiting linear coupling. These materials have recently drawn increasing interest due to their potential applications in multifunctional devices, such as energy harvesters, nonvolatile memory elements, magnetic field sensors, and actuators, ferroelectric photovoltaic, etc. [1, 3]. Few composite (single-phase) multiferroic materials, like Cr_2O_3 or BiFeO_3 , show an important magneto-electric effect, which refers to their capability of coupling the electric and magnetic fields. Since single-phase materials generally have a low magneto-electric effect and their operating temperatures are often below the room temperature, Suchtelen et al. introduced the idea of two-phase composites containing both piezoelectric and piezomagnetic phases, which exhibit the magneto-electric couplings as a product property via stress/strain [4]. These multiphases MEE materials show improved coupling properties compared to single-phase multiferroics. Initiating from this idea, extensive research has been carried out on MEE composite materials. Hamdi et al. [5] studied the Lamb wave propagation in bi-layer piezoelectric/piezomagnetic plates. It was found that a higher thickness ratio is associated with a higher magneto-electromechanical coupling factor for S_0 Lamb mode at low frequency. Xiaoming et al. [6] studied the properties of evanescent Lamb waves in functionally graded piezoelectric-piezomagnetic plates. Almeyda et al. [7] studied the impact of an imperfect interface on the magneto-electro-elastic properties for fiber-reinforced composites. Xiaoming et al. [8] predicted the full dispersion curve of guided waves in functionally graded piezoelectric plates. For



layered magneto-electro-elastic structures subjected to static loads, Pan [9] presented an exact solution for simply supported plates, which was implemented by Pan and Heyliger [10] for the case of cylindrical bending. Xin et al. [11] analyzed the free vibration of layered magneto-electro-elastic beams, whereby it was concluded that the thickness ratio affects greatly the natural frequency for higher mode. Based on an equivalent single-layer model, Alaimo et al. [12] derived an original FE formulation for the analysis of large deflections in MEE multilayered plates. Jiangong et al. studied the dispersion behavior of waves in a layered magneto-electro-elastic plate based on the Legendre polynomial approach [13]. Yu et al. [14] proposed a double orthogonal polynomial series approach to solve the wave propagation problem in a two-dimensional (2-D) multilayered piezoelectric–piezomagnetic bar with rectangular cross-sections. Nonlinear and linear free vibration of symmetrically laminated magneto-electro-elastic doubly-curved thin shell resting on an elastic foundation was studied analytically by Shooshtari et al. [15]. Using the modified couple stress theory, the free vibration of sandwich composite micro-plates (SCMP) made of five smart layers was evaluated by Arani et al. [16]. The literature survey in this section shows that several researchers have studied the multilayer magneto-electro-elastic plates. However, little attention has been paid to study the effect of anisotropy of piezoelectric and piezomagnetic material on the dynamic responses of laminated magneto-electro-elastic plates. With the aid of the partial wave technique in combination with the stiffness matrix method (SMM), the main goal of the current research is to study the influence of the variation of propagation direction on the phase velocity and natural frequency of Lamb waves. Also, different numerical studies are conducted to investigate the effects of different magneto-electric boundary conditions on the dynamic response of multilayer magneto-electro-elastic plates. The variation of the piezoelectric-piezomagnetic axis (from crystallographic basis to working basis) mathematically results in a change in the elastic, piezoelectric, and piezomagnetic tensors. In this context, an analytical solution is presented in this paper to determine the mechanical, piezoelectric, piezomagnetic, and magneto-electric tensors at any polarization orientation. The significance of this work emerges from that the analytical solution developed to determine the different elastic, piezoelectric, and piezomagnetic tensors in the case of fully anisotropic material (monoclinic), can be applied to any other arbitrary symmetry. Otherwise, this research work studies the impact of the anisotropy of the multilayer piezoelectric-piezomagnetic material on phase velocity and natural frequency.

2. Problem Description and Basic Formulation

A set of N anisotropic layers are considered to be stacked normally along the y axis in the rectangular Cartesian coordinates (x, y, z) system, as illustrated in Fig. 1. The total thickness is h , and each layer is parallel to the (x - z) plane and is thickness 1 mm. The multilayer is made of a PZT-5H piezoelectric layer and a piezomagnetic CoFe_2O_4 layer with the material properties given below. Here the thicknesses of the piezoelectric and piezomagnetic layers are denoted by ' h_e ' and ' h_m ', respectively.

Out of the orthotropic axis (monoclinic symmetry) of the layer j , the behavior laws of magneto-electro-elastic materials are [19]:

$$\begin{pmatrix} \sigma_{xx} \\ \sigma_{yy} \\ \sigma_{zz} \\ \sigma_{yz} \\ \sigma_{xz} \\ \sigma_{xy} \end{pmatrix} = [C] \begin{pmatrix} \varepsilon_{xx} \\ \varepsilon_{yy} \\ \varepsilon_{zz} \\ 2\gamma_{yz} \\ 2\gamma_{xz} \\ 2\gamma_{xy} \end{pmatrix} - [e] \begin{pmatrix} E_x \\ E_y \\ E_z \end{pmatrix} - [q] \begin{pmatrix} H_x \\ H_y \\ H_z \end{pmatrix} \quad (1.a)$$

$$\begin{pmatrix} D_x \\ D_y \\ D_z \end{pmatrix} = [e^T] \begin{pmatrix} \varepsilon_{xx} \\ \varepsilon_{yy} \\ \varepsilon_{zz} \\ 2\gamma_{yz} \\ 2\gamma_{xz} \\ 2\gamma_{xy} \end{pmatrix} - [\varepsilon] \begin{pmatrix} E_x \\ E_y \\ E_z \end{pmatrix} + [d] \begin{pmatrix} H_x \\ H_y \\ H_z \end{pmatrix} \quad (1.b)$$

Table 1. Material parameters of the piezoelectric and piezomagnetic materials [17, 18]

	PZT5H	CoFe ₂ O ₄
C_{11} (x10 ⁹ N/m ²)	151	286
C_{12} (x10 ⁹ N/m ²)	98	173
C_{13} (x10 ⁹ N/m ²)	96	170.5
C_{33} (x10 ⁹ N/m ²)	124	269.5
C_{44} (x10 ⁹ N/m ²)	23	45.3
ε_{11} (10 ⁻⁹ Fm ⁻¹)	15	0.08
ε_{33} (10 ⁻⁹ Fm ⁻¹)	13.27	0.093
μ_{11} (10 ⁻⁶ Ns ² C ⁻²)	5	157
μ_{33} (10 ⁻⁶ Ns ² C ⁻²)	1	590
e_{31} (C m ⁻²)	-5.1	-
e_{15} (C m ⁻²)	17	-
e_{33} (C m ⁻²)	27	-
f_{15} (NA ⁻¹ m ⁻¹)	-	550
f_{31} (NA ⁻¹ m ⁻¹)	-	580.3
f_{33} (NA ⁻¹ m ⁻¹)	-	699.7
ρ (10 ³ Kg/m ³)	7.5	5.3



$$\begin{pmatrix} B_x \\ B_y \\ B_z \end{pmatrix} = [q^T] \begin{pmatrix} \epsilon_{xx} \\ \epsilon_{yy} \\ \epsilon_{zz} \\ 2\gamma_{yz} \\ 2\gamma_{xz} \\ 2\gamma_{xy} \end{pmatrix} + [d] \begin{pmatrix} E_x \\ E_y \\ E_z \end{pmatrix} + [\mu] \begin{pmatrix} H_x \\ H_y \\ H_z \end{pmatrix} \tag{1.c}$$

$$\begin{pmatrix} C_{11} & C_{12} & C_{13} & 0 & 0 & C_{16} \\ C_{12} & C_{22} & C_{23} & 0 & 0 & C_{26} \\ C_{13} & C_{23} & C_{33} & 0 & 0 & C_{36} \\ 0 & 0 & 0 & C_{44} & C_{45} & 0 \\ 0 & 0 & 0 & C_{45} & C_{55} & 0 \\ C_{16} & C_{26} & C_{36} & 0 & 0 & C_{66} \end{pmatrix} \quad \begin{pmatrix} 0 & 0 & q_{31} \\ 0 & 0 & q_{32} \\ 0 & 0 & q_{33} \\ q_{14} & q_{24} & 0 \\ q_{15} & q_{25} & 0 \\ 0 & 0 & q_{36} \end{pmatrix} \tag{2}$$

$$\begin{pmatrix} \epsilon_{11} & \epsilon_{12} & 0 \\ \epsilon_{12} & \epsilon_{22} & 0 \\ 0 & 0 & \epsilon_{33} \end{pmatrix} \quad \begin{pmatrix} d_{11} & d_{12} & 0 \\ d_{12} & d_{22} & 0 \\ 0 & 0 & d_{33} \end{pmatrix} \quad \begin{pmatrix} \mu_{11} & \mu_{12} & 0 \\ \mu_{12} & \mu_{22} & 0 \\ 0 & 0 & \mu_{33} \end{pmatrix} \tag{3}$$

In these relationships, (D_x, D_y, D_z) , and (B_x, B_y, B_z) are the components of the electric displacement and magnetic induction, respectively. The parameters (E_x, E_y, E_z) and (H_x, H_y, H_z) are the components of the electric and magnetic fields, respectively. The terms $[C]$ $[e]$ and $[q]$ are the stiffness, piezoelectric, and piezomagnetic tensors, respectively. The terms $[\epsilon]$ $[d]$ and $[\mu]$ are the permittivity, the permeability, and the magnetoelectric tensors, respectively.

In anisotropic materials, the elements of the tensors depend on the orthonormal reference chosen. Depending on the orientation of the axes (planes of symmetry) the material can behave differently in different directions. To obtain the elements of these tensors in the new base, the tensors are rotated. The coordinate system associated with the j^{th} layer is $R_1 = (O, x', y', z')$, and the Cartesian coordinate system associated with the multilayered plate is $R_2 = (O, x, y, z)$. The coordinate system R_1 is the image of the coordinate system R_2 by the angle of rotation θ around the axis (O, z) . The transition matrix from the base system (x', y', z') to the Cartesian basis (x, y, z) is given by:

$$P = \begin{pmatrix} \cos\theta & \sin\theta & 0 \\ -\sin\theta & \cos\theta & 0 \\ 0 & 0 & 1 \end{pmatrix} \tag{4}$$

where P is the rotation matrix. The stress and strain matrix can be transformed from the local to the working basis by [20-22]:

$$\tau_2 = M \tau_1 \tag{5}$$

$$\gamma_2 = M^T \gamma_1 \tag{6}$$

where τ_2 and γ_2 are the tensors of stresses and displacements, respectively, in the (x, y, z) basis. τ_1 and γ_1 are the tensors of stresses and displacements, respectively, in the (x', y', z') basis. With the stress transformation matrix M can be written as follows [20-22]:

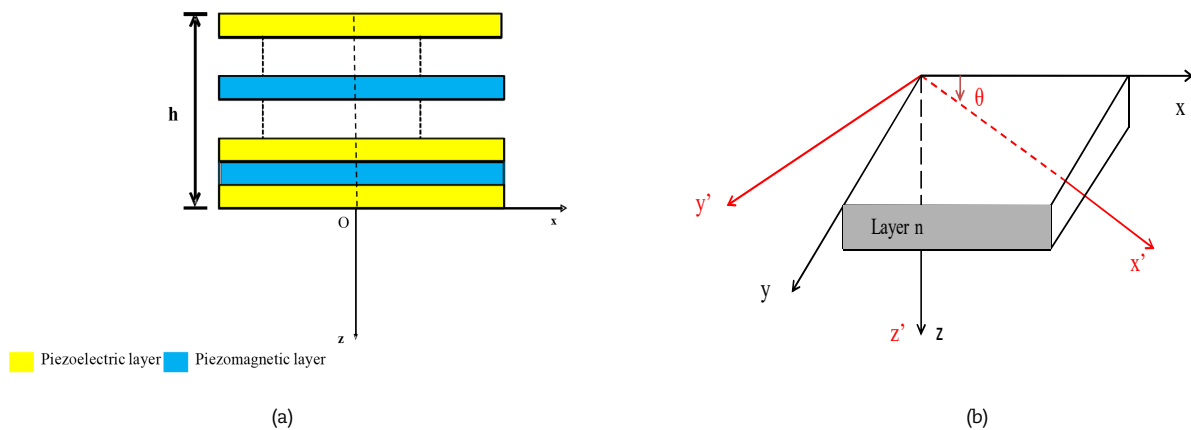


Fig. 1. (a) Schematic of the multilayer MEE plate under working basis (b), the model of the anisotropic piezoelectric or piezomagnetic n^{th} layer.



$$\begin{pmatrix} (\cos \theta)^2 & (\sin \theta)^2 & 0 & 0 & 0 & 2 \sin \theta \cos \theta \\ (\sin \theta)^2 & (\cos \theta)^2 & 0 & 0 & 0 & -2 \sin \theta \cos \theta \\ 0 & 0 & 1 & 0 & 0 & 0 \\ 0 & 0 & 0 & \cos \theta & -\sin \theta & 0 \\ 0 & 0 & 0 & \sin \theta & \cos \theta & 0 \\ -\sin \theta \cos \theta & \sin \theta \cos \theta & 0 & 0 & 0 & (\cos \theta)^2 - (\sin \theta)^2 \end{pmatrix} \quad (7)$$

The magneto-electro-elastic tensor can be transformed from the local to working coordinate system by:

$$[C'] = M[C]M^T ; [q'] = M[q]P ; [\mu'] = P^T[\mu]P \quad (8)$$

$$[e'] = M[e]P ; [\varepsilon'] = P^T[\varepsilon]P ; [d'] = P^T[d]P \quad (9)$$

with the superscript T is the transposed matrix. By developing the equations (8) and (9) we obtain in the Cartesian coordinate system R_2 the tensors $[C']$ $[q']$ $[e']$ $[d']$ $[\varepsilon']$, and $[\mu']$ in the working basis at any orientation angle as follows:

$$\begin{cases} C'_{11} = (\cos \theta)^4 C_{11} + (\sin \theta)^4 C_{22} + 2(C_{12} + 2C_{66})(\sin \theta \cos \theta)^2 \\ C'_{22} = (\sin \theta)^4 C_{11} + (\cos \theta)^4 C_{22} + 2(C_{12} + 2C_{66})(\sin \theta \cos \theta)^2 \\ C'_{33} = C_{33} \\ C'_{44} = (\cos \theta)^2 C_{44} + (\sin \theta)^2 C_{55} \\ \mu'_{12} = (\mu_{11} - \mu_{22}) \sin \theta \cos \theta \\ C'_{66} = ((\cos \theta)^4 + (\sin \theta)^4) C_{66} + (C_{11} + C_{22} - 2(C_{12} + C_{66}))(\sin \theta \cos \theta)^2 \\ C'_{12} = ((\cos \theta)^4 + (\sin \theta)^4) C_{12} + (C_{11} + C_{22} - 4C_{66})(\sin \theta \cos \theta)^2 \\ C'_{13} = (\cos \theta)^2 C_{13} + (\sin \theta)^2 C_{23} \\ C'_{23} = (\sin \theta)^2 C_{13} + (\cos \theta)^2 C_{23} \\ C'_{45} = (C_{44} - C_{55}) \sin \theta \cos \theta \\ C'_{16} = \cos^3 \theta \sin \theta (C_{12} - C_{11} + 2C_{66}) + (C_{22} - C_{12} - 2C_{66}) \cos \theta \sin^3 \theta \\ C'_{26} = \cos^3 \theta \sin \theta (-C_{12} + C_{22} - 2C_{66}) + (-C_{22} + C_{12} + 2C_{66}) \cos \theta \sin^3 \theta \\ C'_{36} = (C_{23} - C_{13}) \sin \theta \cos \theta \end{cases}$$

$$\begin{cases} e'_{14} = -e'_{25} = -(e_{15} + e_{24}) \sin \theta \cos \theta \\ e'_{24} = e_{24} (\cos^2 \theta) - e_{15} (\sin^2 \theta) \\ e'_{15} = e_{15} (\cos^2 \theta) - e_{24} (\sin^2 \theta) \\ e'_{31} = e_{31} (\cos^2 \theta) + e_{32} (\sin^2 \theta) \\ e'_{32} = e_{31} (\sin^2 \theta) + e_{32} (\cos^2 \theta) \\ e'_{33} = e_{33} \\ e'_{36} = (e_{32} - e_{31}) \sin \theta \cos \theta \end{cases}$$

$$\begin{cases} \varepsilon'_{11} = \varepsilon_{11} (\cos^2 \theta) + \varepsilon_{22} (\sin^2 \theta) \\ \varepsilon'_{22} = \varepsilon_{22} (\cos^2 \theta) + \varepsilon_{11} (\sin^2 \theta) \\ \varepsilon'_{33} = \varepsilon_{33} \\ \varepsilon'_{12} = (\varepsilon_{11} - \varepsilon_{22}) \sin \theta \cos \theta \end{cases}$$

$$\begin{cases} \mu'_{11} = \mu_{11} (\cos^2 \theta) + \mu_{22} (\sin^2 \theta) \\ \mu'_{22} = \mu_{22} (\cos^2 \theta) + \mu_{11} (\sin^2 \theta) \\ \mu'_{33} = \mu_{33} \\ \mu'_{12} = (\mu_{11} - \mu_{22}) \sin \theta \cos \theta \end{cases}$$

$$\begin{cases} d'_{11} = d_{11} (\sin^2 \theta) + d_{22} (\cos^2 \theta) \\ d'_{22} = d_{22} (\cos^2 \theta) + d_{11} (\sin^2 \theta) \\ d'_{33} = d_{33} \\ d'_{12} = (d_{11} - d_{22}) \sin \theta \cos \theta \end{cases}$$



$$\begin{cases} \dot{q}_{14} = -\dot{q}_{25} = -(q_{15} + q_{24})\sin\theta\cos\theta \\ \dot{q}_{24} = q_{24}(\cos^2\theta) - q_{15}(\sin^2\theta) \\ \dot{q}_{15} = q_{15}(\cos^2\theta) - q_{24}(\sin^2\theta) \\ \dot{q}_{31} = q_{31}(\cos^2\theta) - q_{32}(\sin^2\theta) \\ \dot{q}_{32} = q_{31}(\sin^2\theta) + q_{32}(\cos^2\theta) \\ \dot{q}_{33} = q_{33} \\ \dot{q}_{36} = (q_{32} - q_{31})\sin\theta\cos\theta \end{cases}$$

As mentioned previously, we will study a structure made up of materials of hexagonal symmetry (transversely isotropic). For hexagonal symmetry, Lamb and SH mode are decoupled only for 0 and 90 degrees [23].

3. The Stiffness Matrix Approach (SMA)

Without any loss of generality, a bi-layer piezoelectric-piezomagnetic plate can be considered to illustrate the assembly of the global matrix method as shown in Fig. 2. The interface between the two-layers is supposed to be perfectly bounded.

The unknown eigenvalues and eigenvectors are computed using the ordinary differential equation (ODE). As this method is developed in the previous work, further details can be obtained from this reference [24]. At the interface $z = 0$, the stress matrix noted by τ and the displacements matrix noted by u can be written as follows [25, 26]:

$$\begin{bmatrix} u_0^+ \\ u_0^- \end{bmatrix} = \begin{bmatrix} P^+ & P^-H^- \\ P^+H^+ & P^- \end{bmatrix} \begin{bmatrix} A^+ \\ A^- \end{bmatrix} \tag{10}$$

$$\begin{bmatrix} \tau_0^+ \\ \tau_0^- \end{bmatrix} = \begin{bmatrix} D^+ & D^-H^- \\ D^+H^+ & D^- \end{bmatrix} \begin{bmatrix} A^+ \\ A^- \end{bmatrix} \tag{11}$$

with $p^\pm (4 \times 4) = (p_1^\pm, p_2^\pm, p_3^\pm, p_4^\pm)$ are the polarization matrices and $H^\pm (4 \times 4)$ are the diagonal phase shift matrices which are written in the following form:

$$\begin{aligned} H^+ (4 \times 4) &= \text{Diag}(e^{ik_z^{1h}}, e^{ik_z^{2h}}, e^{ik_z^{3h}}, e^{ik_z^{4h}}) \\ H^- (4 \times 4) &= \text{Diag}(e^{ik_z^{1h}}, e^{ik_z^{2h}}, e^{ik_z^{3h}}, e^{ik_z^{4h}}) \end{aligned} \tag{12}$$

$D^\pm (4 \times 4) = (d_1^\pm, d_2^\pm, d_3^\pm, d_4^\pm)$ is the stress matrix. The components (d_i^\pm) , of (d^\pm) , vector are related to the polarization vector (p^\pm) , by: $(d_n^\pm)_j = (C_{13kl}k_k p_l^\pm)_j$. The local stiffness matrices of two neighboring layers are considered. The combinations of these two matrices give below:

$$\begin{bmatrix} \tau_1 \\ \tau_2 \end{bmatrix} = \begin{bmatrix} K_{11}^A & K_{12}^A \\ K_{21}^A & K_{22}^A \end{bmatrix} \begin{bmatrix} u_1 \\ u_2 \end{bmatrix} \tag{13}$$

$$\begin{bmatrix} \tau_2 \\ \tau_3 \end{bmatrix} = \begin{bmatrix} K_{11}^B & K_{12}^B \\ K_{21}^B & K_{22}^B \end{bmatrix} \begin{bmatrix} u_2 \\ u_3 \end{bmatrix} \tag{14}$$

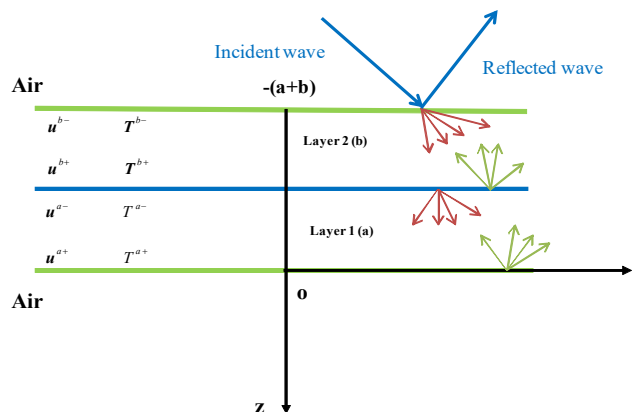


Fig. 2. Schematic of a bi-layer piezoelectric-piezomagnetic plate.



Combining (13) and (14):

$$K^{a,b} = \begin{bmatrix} K_{11}^A + K_{12}^A (K_{11}^B - K_{22}^A)^{-1} K_{21}^A & -K_{21}^A (K_{11}^B - K_{22}^A)^{-1} K_{12}^B \\ K_{21}^B (K_{11}^B - K_{22}^A)^{-1} K_{21}^A & K_{22}^B - K_{21}^B (K_{11}^B - K_{22}^A)^{-1} K_{12}^B \end{bmatrix} \quad (15)$$

So the stiffness matrix relating the stress at the bottom and at the top of the bi-layer is written as:

$$K^{a,b} = \begin{bmatrix} K_{11}^A + K_{12}^A (K_{11}^B - K_{22}^A)^{-1} K_{21}^A & -K_{21}^A (K_{11}^B - K_{22}^A)^{-1} K_{12}^B \\ K_{21}^B (K_{11}^B - K_{22}^A)^{-1} K_{21}^A & K_{22}^B - K_{21}^B (K_{11}^B - K_{22}^A)^{-1} K_{12}^B \end{bmatrix} \quad (16)$$

By recurrence the stiffness matrix of the multilayer from the bottom $z=-h$ to the top $z=h$ is written as follows:

$$\begin{bmatrix} \tau_{-h} \\ \tau_0 \end{bmatrix} \begin{bmatrix} K_{11} & K_{12} \\ K_{21} & K_{22} \end{bmatrix}^N \begin{bmatrix} u_{-h} \\ u_0 \end{bmatrix} \quad (17)$$

Developing Eq. (17) we obtain:

$$\begin{aligned} U_{-h} &= (K_{21}^N)^{-1} (T_0 - K_{22}^N U_0) \\ T_{-h} &= (K_{21}^N - K_{11}^N (K_{21}^N)^{-1} K_{22}^N) U_0 + K_{11}^N (K_{21}^N)^{-1} T_0 \end{aligned} \quad (18)$$

By imposing the mechanical, electrical and magnetic boundary conditions at the upper and lower surfaces of the multilayer, two cases of magneto-electric boundary conditions are established in this study [27, 28]:

Electrically open circuit and magnetically short circuit boundary conditions (noted os) at both free surfaces at $z=0$ and $z=-h$:

$$\tau_{13} = \tau_{33} = D_3 = B_3 = 0 \quad (19)$$

Electrical short circuit and magnetic open circuit condition (noted so) at both free surfaces at $z=0$ and $z=-h$:

$$\tau_{13} = \tau_{33} = \phi = \psi = 0 \quad (20)$$

At this stage, knowing the stress and displacement matrix at the upper and lower interfaces of the multilayer, two (8x8) matrixes are then constructed in magneto-electrical open and short circuit conditions.

$$\begin{pmatrix} u_1 \\ u_3 \\ \phi \\ \psi \\ T_{13} \\ T_{33} \\ D_3 \\ B_3 \end{pmatrix}_0 = \begin{pmatrix} Q_{11}^{os} & Q_{12}^{os} \\ Q_{21}^{os} & Q_{22}^{os} \end{pmatrix} \begin{pmatrix} u_1 \\ u_3 \\ \phi \\ \psi \\ T_{13} \\ T_{33} \\ D_3 \\ B_3 \end{pmatrix}_{-h} \quad (21)$$

$$\begin{pmatrix} u_1 \\ u_3 \\ D_3 \\ B_3 \\ T_{13} \\ T_{33} \\ \phi \\ \psi \end{pmatrix}_0 = \begin{pmatrix} Q_{11}^{so} & Q_{12}^{so} \\ Q_{21}^{so} & Q_{22}^{so} \end{pmatrix} \begin{pmatrix} u_1 \\ u_3 \\ D_3 \\ B_3 \\ T_{13} \\ T_{33} \\ \phi \\ \psi \end{pmatrix}_{-h} \quad (22)$$

In order to obtain the nontrivial solutions of the above equations (Eqs. 21 and 22), the determinant of $Q_{21}^{os,so}$ must vanish. So, the dispersive behaviors for the magneto-electrical open and short circuit cases can be investigated.

4. Results and Discussions

Before studying the problem of the propagation of the ultrasonic waves in multilayer piezoelectric-piezomagnetic material, we verify our theoretical approach by comparing the present results with those of a previous work of Chen et al. [29]. The natural



frequency is normalized as follows: $\Omega = \omega H / \sqrt{C_{max} / \rho_{max}}$. Table 1 presents the natural frequencies at $kh=2$ for the first five guided modes of the multilayer magneto-electro-elastic material (the fundamental Lamb mode A_0 and S_0 , the fundamental shear horizontal wave SH_0 , the first higher antisymmetric Lamb mode A_1 and the first higher shear horizontal mode SH_1). ‘B’ refers to the piezoelectric layer $BaTiO_3$, and ‘F’ refers to piezomagnetic layer $CoFe_2O_4$. The present results are compared with those of Chen. The relative error is found to be very small, and it was less than 1%. This can make the general stiffness matrix method highly suitable for predicting the response of a multilayer magneto-electro-elastic material subjected to an excitation.

4.1. Effect of polarization direction on natural frequency.

In this section, the effect of the anisotropy of the multilayer magneto-electro-elastic material on the natural frequency of the first four Lamb modes at $kh=2$ is studied. ‘B’ refers to the piezoelectric layer PZT-5H, and ‘F’ refers to the piezomagnetic layer $CoFe_2O_4$.

Table 2. Validation study

Laminate		Mode				
		A_0	SH_0	S_0	SH_1	A_1
B/B/B	Chen [28]	0.7224	1.0355	1.7471	1.9049	2.5497
	Present	0.7223	1.0355	1.7470	1.9049	2.5495
	Relative error (%)	0.0138	-	0.0057	-	0.0078
F/F/F	Chen [28]	0.5614	0.8889	1.4462	1.5341	1.9824
	Present	0.5648	0.8889	1.4493	1.5341	1.9915
	Relative error (%)	0.6019	-	0.2139	-	0.4569
B/F/B	Chen [28]	0.5453	0.8349	1.4105	1.4741	1.9174
	Present	0.5471	0.8348	1.4117	1.4740	1.9243
	Relative error (%)	0.3290	0.0119	0.0850	0.0067	0.3585
F/B/F	Chen [28]	0.5943	0.8817	1.4564	1.5798	2.1196
	Present	0.5962	0.8817	1.4581	1.5798	2.0974
	Relative error (%)	0.3186	-	0.1165	-	1.0474
B/B/F	Chen [28]	0.5710	0.8324	1.3906	1.5171	2.0316
	Present	0.5719	0.8324	1.3913	1.5171	2.0338
	Relative error (%)	0.1573	-	0.0503	-	0.1081
F/F/B	Chen [28]	0.5655	0.8790	1.4567	1.5415	1.9965
	Present	0.5680	0.8790	1.4588	1.5415	2.0032
	Relative error (%)	0.4401	-	0.1439	-	0.3344

Table 3. Dimensionless natural frequencies at $kh=2$

Laminate	Polarization	Mode			
		A_0	S_0	A_1	S_1
B/B/B	$0^\circ / 0^\circ / 0^\circ$	0.6702	1.4967	2.1956	2.5387
	$0^\circ / 90^\circ / 0^\circ$	0.7002	1.6288	2.4850	3.0015
	$90^\circ / 0^\circ / 90^\circ$	0.5352	1.5528	2.1338	2.8899
	$90^\circ / 90^\circ / 90^\circ$	0.5598	1.8933	2.6815	3.2035
F/F/F	$0^\circ / 0^\circ / 0^\circ$	0.5648	1.4493	1.9915	2.5660
	$90^\circ / 90^\circ / 90^\circ$	0.5730	1.4680	1.9996	2.6575
B/F/B	$0^\circ / 0^\circ / 0^\circ$	0.5215	1.3436	1.7196	2.3433
	$0^\circ / 0^\circ / 90^\circ$	0.5256	1.3695	1.7831	2.3580
F/B/F	$90^\circ / 90^\circ / 90^\circ$	0.5453	1.4345	1.9021	2.4574
	$0^\circ / 0^\circ / 0^\circ$	0.6202	1.4456	2.2812	2.6791
B/B/F	$0^\circ / 90^\circ / 0^\circ$	0.6160	1.4976	2.2865	2.7716
	$0^\circ / 0^\circ / 0^\circ$	0.5460	1.2162	1.9043	2.2564
	$0^\circ / 90^\circ / 0^\circ$	0.5329	1.2087	1.9104	2.4422
F/F/B	$90^\circ / 90^\circ / 90^\circ$	0.5284	1.3776	2.0436	2.5146
	$0^\circ / 0^\circ / 0^\circ$	0.5893	1.4499	2.0663	2.7197
	$0^\circ / 0^\circ / 90^\circ$	0.5955	1.5058	2.1262	2.7117



We consider orientations at $\theta = 0^\circ$ and $\theta = 90^\circ$, as shown in Table 3. The natural frequencies at $kh=2$ for different stacking sequences (F/F/F, B/B/B, B/F/B, F/B/F, B/B/F, F/F/B) and different orientation directions are then computed. As shown in Table 3, the natural frequency changes (increases or decreases) with the variation of the polarization direction. For the pure piezomagnetic multilayer F/F/F, the variation of orientation angle causes slight change in the value of the natural frequency compared to the other stacking sequences. One important information from Table 3 is that the variation of the piezoelectric A_6 axis always has the most significant effect on the natural frequency compared to the A_6 piezomagnetic axis, whose effect is very small in the purely piezomagnetic multilayer and negligible in the multilayer piezoelectric-piezomagnetic material. We notice also that the purely piezoelectric multilayer has a higher natural frequency compared to those of the multilayers develop from other stacking sequences. Furthermore, Fig. 3 shows the non-dimensional frequency versus the non-dimensional wave-number for all stacking sequences of the multilayer. The effect of anisotropy is studied in this section for the two fundamental S_0 and A_0 Lamb modes. From Fig. 3 we can see the greatest influence of the variation of the crystallographic axis on the dynamic response of the piezoelectric-piezomagnetic multilayer. Fig. 3 shows that in the case of purely piezoelectric multilayer B/B/B, the variation of the polarization direction has a great impact on the non-dimensional frequency. However, for the purely piezomagnetic multilayer F/F/F, the variation of the piezomagnetic A_6 axis has a weak influence on the A_0 and S_0 modes except at high wave-number for the S_0 mode when the variation of the non-dimensional frequency becomes important. For the multilayer piezoelectric-piezomagnetic stacking sequences, it is noted that for F/F/B and F/B/F stacking sequences, only the variation of the A_6 piezoelectric axis changes the non-dimensional frequency. For B/B/F and B/F/B stacking sequences where the piezoelectric phase is predominant, the $(90^\circ/90^\circ/90^\circ)$ orientation highly affects the non-dimensional frequency, especially for the S_0 mode.

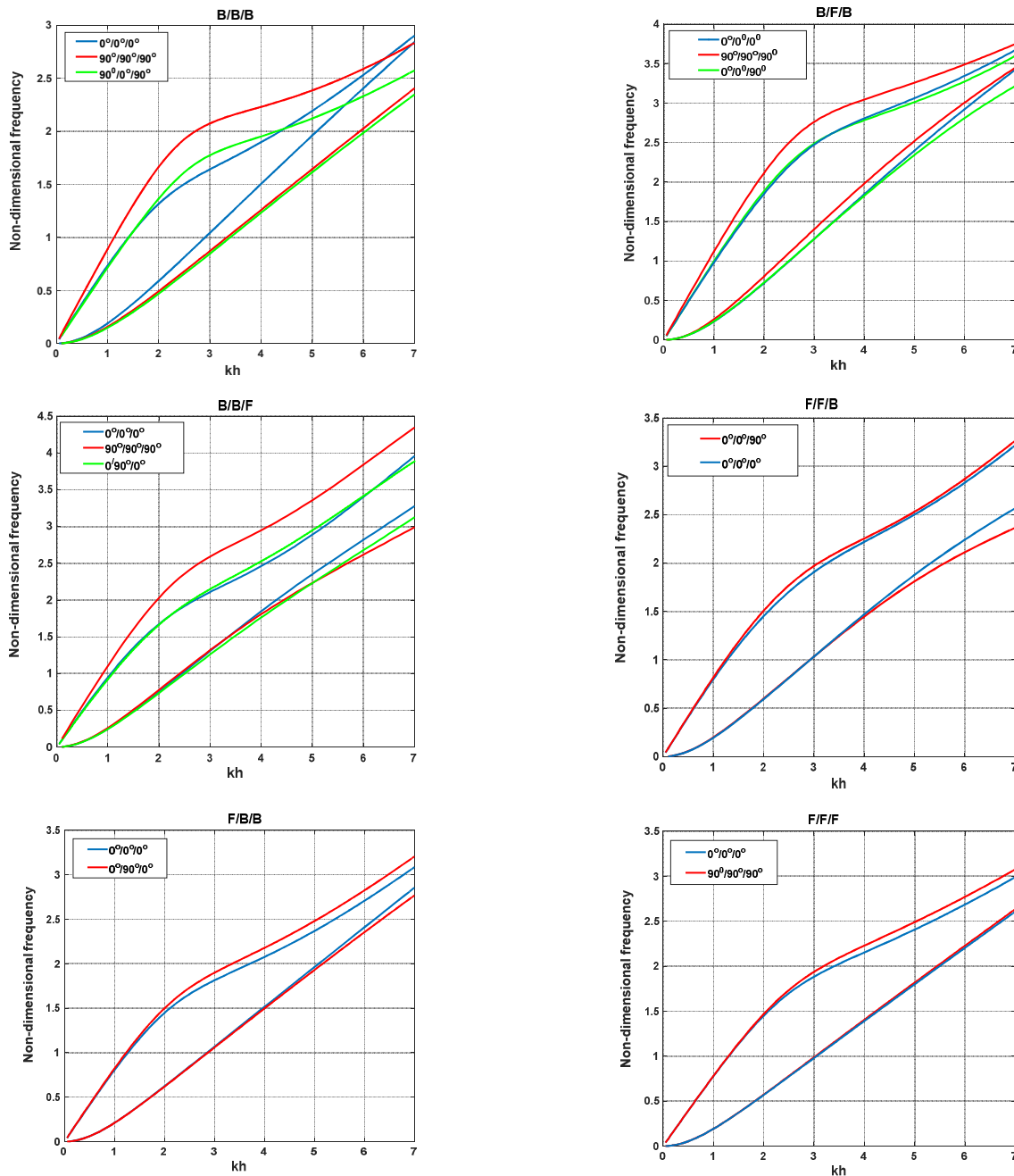


Fig. 3. Variation of non-dimensional frequency with non-dimensional wave-number for different stacking sequences and orientation direction for the multilayer material.



Table 4. Dimensionless natural frequencies Ω at $kh=2$ for different magneto-electric boundary conditions

Laminate	Magneto-electric Boundary Condition	Mode			
		A_0	S_0	A_1	S_1
B/B/B	so	0.6519	1.2743	1.8656	2.5086
	os	0.6582	1.3917	2.0039	2.5316
F/F/F	so	0.5639	1.4493	1.9909	2.5664
	os	0.5643	1.4494	1.9912	2.5664
B/F/B	so	0.5149	1.3009	1.5458	2.1397
	os	0.5182	1.3185	1.6251	2.2517
F/B/F	so	0.6187	1.4452	2.2774	2.6785
	os	0.6194	1.4454	2.2793	2.6788
B/B/F	so	0.5347	1.1225	1.7310	2.2545
	os	0.5455	1.2161	1.9030	2.2563
F/F/B	so	0.5857	1.3887	1.9454	2.6325
	os	0.5862	1.3889	1.9455	2.6327

4.2. Effect of magneto-electric boundary condition on natural frequency

Table 4 shows the effect of the magneto-electric boundary conditions defined above on the natural frequency of the different stacking sequences of the magneto-electro-elastic multilayer material. It can be noticed from the results of Table 4 that the magnetic-electric boundary condition has a significant influence on the natural frequency, except in the case of a purely multilayer piezomagnetic material where the influence is very small. We can also notice that in the case of (os) magneto-electric boundary conditions whereby the electric and magnetic scalar potential vanishes on the free surface, the natural frequency decreases.

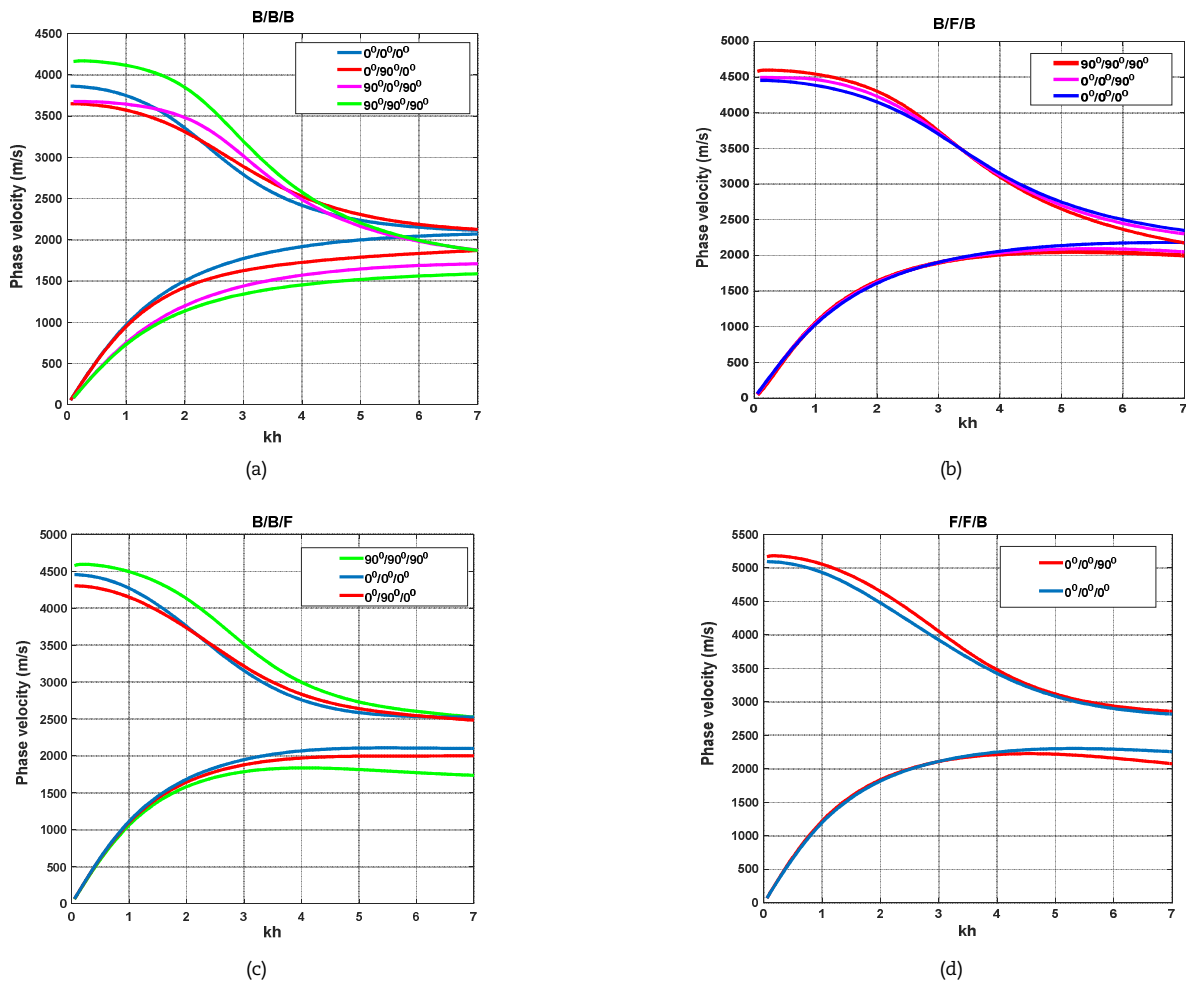


Fig. 4. Phase velocity versus non-dimensional wave-number of different crystallographic orientation.



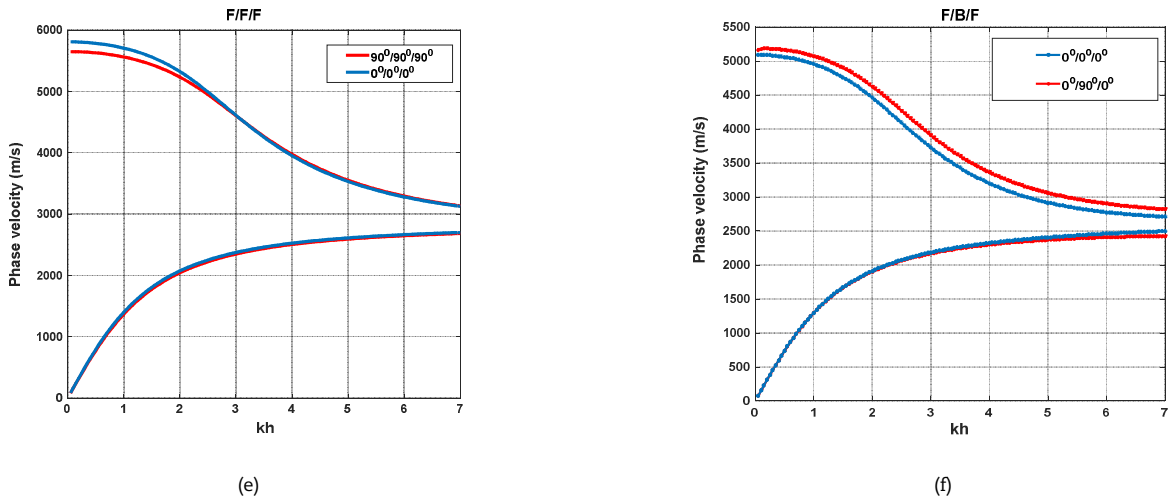


Fig. 4. Continued.

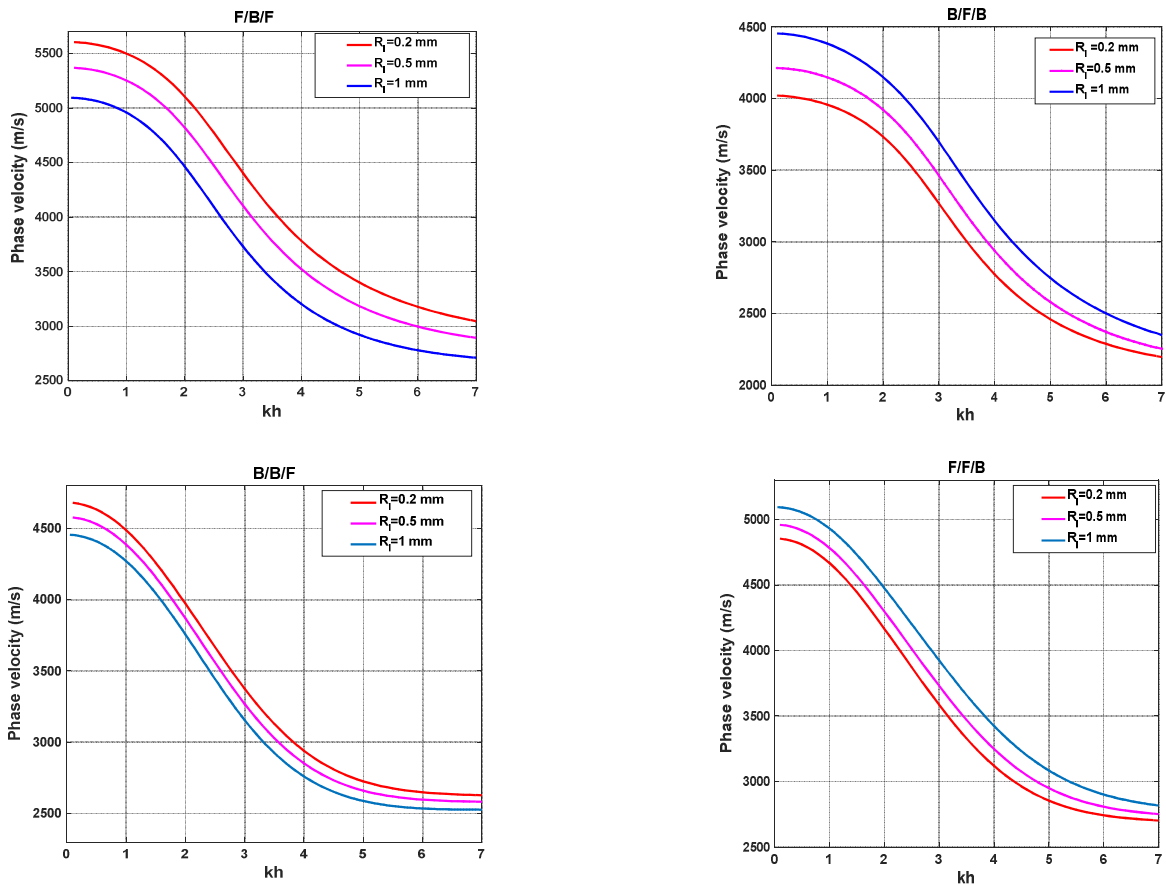


Fig. 5. Variation of the phase velocity with the non-dimensional wave-number of the fundamental S_0 mode for different interlayer thicknesses.

4.3. Effect of anisotropy on dispersion curve

In this section, we study the effect of the variation of piezoelectric and piezomagnetic A_6 axis on the phase velocity of the two fundamental Lamb modes. We focused the investigation on A_0 and S_0 Lamb waves because of their major practical application in non-destructive technology (NDT). As shown in Fig. 4, the phase velocity highly depends on the orientation of crystallographic axis A_6 , it increases or decreases with the non-dimensional wave-number kh . For the purely piezoelectric B/B/B multilayer material, the variation of the piezoelectric fiber highly affects both anti-symmetric and symmetric modes, compared with the purely piezomagnetic F/F/F multilayer material, where by the variation of the piezomagnetic fiber at $\theta = 90^\circ$ slightly affects the fundamental symmetric mode at low wave-number range.

During this study, we noticed that only the piezoelectric A_6 axis influences the two fundamental modes, on the other hand the influence of the variation of the piezomagnetic axis is negligible.



4.4. Effect of interlayer thickness on phase velocity

In this section, we denote the interlayer thickness of the multilayer by R_i . In each of the stacking sequences presented below, we study the influence of the variation of the interlayer thickness on the phase velocity of the S_0 Lamb mode. The results are presented in Fig. 5. It is seen that the interlayer thickness considerably affects the S_0 mode. The phase velocity increases as the interlayer thickness decreases in the case of F/B /F and B/B/F. Contrariwise, it decreases with a decrease in the interlayer thickness in the case of B/F/B and F/F/B multilayer structures. It can be summarized that a decrease in the thickness of the piezoelectric intermediate layer increases the phase velocity of the S_0 mode; however, when the interlayer is piezomagnetic, a reduction in thickness decreases the phase velocity of the S_0 mode of the multilayer.

5. Conclusion

The free vibration of multilayer magneto-electro-elastic plates has been analyzed based on an efficient numerical approach; the general stiffness method. A good agreement is found between the present results with those obtained by Chen et al. [29], which validates our numerical approach. The dispersion curves and the natural frequencies of the guided waves with different stacking sequences are investigated for high and low frequencies. It is established that the anisotropy of the piezoelectric and piezomagnetic crystals significantly affects the dispersion and natural frequency responses of the guided waves. The magneto-electric boundary condition has also slight influence on the natural frequency. Furthermore, an important effect of the interlayer thickness on the phase velocity of S_0 mode was found. The knowledge gained from this study is of great importance for NDT applications. The outcomes of the present work will contribute to the design of new acoustic devices based on anisotropic magneto-electro-elastic materials, which are good candidates for the emerging NDT technology.

Author Contributions

Hamdi Ezzin: Planned the scheme, initiated the project, implemented the computer Code and write the original draft, Mohamed Mkaour: Revision editing, Investigation, Zhenghua Qian: Supervision, Funding acquisition, Mohammad Arefi: Visualization, Writing-reviewing and editing, Raj Das: Revision editing, Investigation. The manuscript was written through the contribution of all authors. All authors approved the final version of the manuscript.

Acknowledgments

The authors greatly appreciate the editor and anonymous reviewers who have dedicated their considerable time and expertise to enhance this paper with constructive and valuable comments.

Conflict of Interest

The authors declared no potential conflicts of interest with respect to the research, authorship and publication of this article.

Funding

This work was supported by the National Natural Science Foundation of China: [grant numbers 12061131013, 12172171]; the State Key Laboratory of Mechanics and Control of Mechanical Structures: [grant number MCMS-E-0520K02]; the Fundamental Research Funds for the Central Universities: [grant numbers NE2020002, NS2019007]; National Natural Science Foundation of China for Creative Research Groups [grant number 51921003].

Data Availability Statements

The datasets generated and/or analyzed during the current study are available from the first author on reasonable request.

References


- [1] Priya, S., Islam, R., Dong, S., Viehland, D., Recent advancements in magnetolectric particulate and laminate composites, *Journal of Electroceramics*, 19, 2007, 149–66.
- [2] Nan, C-W., Bichurin, M., Dong, S., Viehland, D., Srinivasan, G., Multiferroic magnetolectric composites: historical perspective, status, and future directions, *Journal of Applied Physics*, 103, 2008, 031101.
- [3] Vopsaroiu, M., Blackburn, J., Cain, M.G., Emerging Technologies and Opportunities Based on the Magneto-Electric Effect in Multiferroic Composites, *Materials Research Society Symposium Proceedings*, 1161, 2009.
- [4] Van Suchtelen, J., Product properties: a new application of composite materials, *Philips Research Reports*, 27(1), 1972, 28–37.
- [5] Ezzin, H., Ben Amor, M., Ben Ghazlen, M.H., Lamb waves propagation in layered piezoelectric/piezomagnetic plates, *Ultrasonics*, 76, 2017, 63–69.
- [6] Zhang, X., Li, Z., Yu, J., The Computation of Complex Dispersion and Properties of Evanescent Lamb Wave in Functionally Graded Piezoelectric-Piezomagnetic Plates, *Materials*, 11, 2018, 1186.
- [7] Espinosa-Almeyda, Y., Camacho-Montes, H., Rodríguez-Ramos, R., R.Guinovart-Díaz J,C, López-Realpozo, J.Bravo-Castillero, Sabina, F.J., Influence of imperfect interface and fiber distribution on the antiplane effective magneto-electro-elastic properties for fiber reinforced composites, *International Journal of Solids and Structures*, 112, 2017, 155-168.
- [8] Zhang, X., Zhang, C., Jiangong, Y., Jing, L., Full dispersion and characteristics of complex guided waves in functionally graded piezoelectric plates, *Journal of Intelligent Material Systems and Structures*, 30(10), 2019, 1466-1480.
- [9] Pan, E., Exact solution for simply supported and multilayered magneto-electro-elastic plates, *Journal of Applied Mechanics*, 68(4), 2001, 608–18.
- [10] Pan, E., Heyliger, P., Exact solutions for magneto-electro-elastic laminates in cylindrical bending, *International Journal of Solids and Structures*, 40, 2003, 6859–76.
- [11] Libo, X., Zhendong, H., Free vibration of layered magneto-electro-elastic beams by SS-DSC approach, *Composite Structures*, 125, 2015, 96-103.
- [12] Alaimo, A., Benedetti, I., Milazzo A., A finite element formulation for large deflection of multilayered magneto-electro-elastic plates, *Composite Structures*, 107, 2014, 643–53.
- [13] Jiangong, Y., Juncai, D., Zhijuan, M., On dispersion relations of waves in multilayered magneto-electro-elastic plates, *Applied Mathematical Modelling*, 36, 2012, 5780–5791.
- [14] Yu, J.G., Lefebvre, E., Zhang, Ch., Guided wave in multilayered piezoelectric-piezomagnetic bars with rectangular cross-sections, *Composite Structures*, 116, 2014, 336-345.





- [15] Shooshtari, A., Soheil R., Linear and nonlinear free vibration of a multilayered magneto-electro-elastic doubly-curved shell on elastic foundation, *Composites Part B: Engineering*, 78(1), 2015, 95-108.
- [16] Ghorbanpour, A., Arania, H., Khani Arania Z, Khoddami M., Vibration analysis of sandwich composite micro-plate under electro-magneto-mechanical loadings, *Applied Mathematical Modelling*, 40, 2016, 10596-10615.
- [17] Kumar, A., Chakraborty, D., Effective properties of thermo-electro-mechanically coupled piezoelectric fiber reinforced composites, *Materials & Design*, 30, 2009, 1216-1222.
- [18] Pang, Y., Gao, J-S., Liu, J-X., SH wave propagation in magnetic–electric periodically layered plates, *Ultrasonics*, 54, 2014, 1341-1349.
- [19] Benveniste, Y., Magnetolectric effect in fibrous composites with piezoelectric and piezomagnetic phases, *Physical Review B*, 51, 1995, 16424.
- [20] Kollár, L.P., Springer, G.S., *Mechanics of composite structures*, Cambridge University Press, New York, 2003.
- [21] Pant, S., Laliberte, J., Martinez, M., Rocha, B., Derivation and experimental validation of Lamb wave equations for an n-layered anisotropic composite laminate, *Composite Structures*, 111, 2014, 566-579.
- [22] Gornet L., *Généralités sur les matériaux composites*, Ph.D. Thesis, Ecole centrale de Nantes, Nantes, 2008.
- [23] Quintanilla, F.H., Lowe, M.J.S., Craster, R.V., Modeling guided elastic waves in generally anisotropic media using a spectral collocation method, *The Journal of the Acoustical Society of America*, 137, 2015, 1180–1194.
- [24] Ezzin, H., Mkaoir, M., Arefi, M., Qian, Z., Das, R., Analysis of guided wave propagation in functionally graded magneto-electro elastic composite, *Waves in Random and Complex Media*, 2021, DOI: 10.1080/17455030.2021.1968541.
- [25] Rokhlin, S.I., Wang, L., Stable recursive algorithm for elastic wave propagation in layered anisotropic media: Stiffness matrix method, *Journal of the Acoustic Society of America*, 112, 2002, 822-34.
- [26] Rokhlin, S.I., Wang, L., Ultrasonic waves in layered anisotropic media: characterization of multidirectional composites, *International Journal of Solids and Structures*, 39, 2002, 5529-45.
- [27] Alshits, V.I., Darinskii, A.N., Lothe, J., On the existence of surface waves in half-infinite anisotropic elastic media with piezoelectric and piezomagnetic properties, *Wave Motion*, 16, 1992, 265-283.
- [28] Ezzin, H., Wang, B., Qian, Z., Propagation behavior of ultrasonic Love waves in functionally graded piezoelectric-piezomagnetic materials with exponential variation, *Mechanics of Materials*, 148, 2020, 103492.
- [29] Chen, J., Pan, E., Chen, H., Wave propagation in magneto-electro-elastic multilayered plates, *International Journal of Solids and Structures*, 44, 2007, 1073-1085.


ORCID iD

Hamdi Ezzin  <https://orcid.org/0000-0003-3679-1353>

Mohamed Mkaoir  <https://orcid.org/0000-0001-7633-1410>

Zhenghua Qian  <https://orcid.org/0000-0003-3400-8361>

Mohammad Arefi  <https://orcid.org/0000-0002-5037-7813>

Raj Das  <https://orcid.org/0000-0001-9977-6201>



© 2022 Shahid Chamran University of Ahvaz, Ahvaz, Iran. This article is an open access article distributed under the terms and conditions of the Creative Commons Attribution-NonCommercial 4.0 International (CC BY-NC 4.0 license) (<http://creativecommons.org/licenses/by-nc/4.0/>).

How to cite this article: Ezzin H., Mkaoir M., Qian Z., Arefi M., Das R. Lamb Wave Analysis in Anisotropic Multilayer Piezoelectric-piezomagnetic Material, *J. Appl. Comput. Mech.*, 8(2), 2022, 629–640. <https://doi.org/10.22055/JACM.2021.38165.3168>

Publisher's Note Shahid Chamran University of Ahvaz remains neutral with regard to jurisdictional claims in published maps and institutional affiliations.

